

OPTIMIZATION OF METHYLENE BLUE DYE REMOVAL BY PEANUT HUSK USING PLACKETT-BURMAN DESIGN AND RESPONSE SURFACE METHODOLOGY

Kah-Tong CHAN^a and Siew-Teng ONG^{a,b,*}

ABSTRACT. The ability of peanut husk in removing Methylene Blue (MB) dye solution was studied in this project. The influence of various factors such as contact time, initial dye concentrations, pH and adsorbent dosage were examined in this project in order to study their effects towards the adsorption process. The percentage uptake of MB increases with contact time, pH and adsorbent dosage while it decreases with increasing initial dye concentrations. The functional group on peanut husk was determined using Fourier Transform Infrared Spectrophotometer (FTIR) and its surface morphology was characterized using Scanning Electron Microscope (SEM) and Atomic Force Microscope (AFM) analysis. The experimental data fitted well into the pseudo-second-order kinetic model with R^2 values close to unity. The experimental data is best fitted with Freundlich isotherm model by having R^2 of 0.9927. By using Plackett-Burman design, the factors that can bring significant impact towards the adsorption of MB by peanut husks were determined to be contact time, pH and adsorbent dosage. The optimum condition for the adsorption process was determined by Response Surface Methodology. It was found that the optimum condition was reached at 120 minutes of contact time, pH 10 and 0.035 g of adsorbent.

Keywords: Adsorption, Methylene Blue, Peanut husk, Plackett-Burman Design, Response Surface Methodology

^a Department of Chemical Science, Faculty of Science, Universiti Tunku Abdul Rahman, Jalan Universiti, Bandar Barat, 31900 Kampar, Perak, Malaysia

^b Centre for Agriculture and Food Research, Universiti Tunku Abdul Rahman, Jalan Universiti, Bandar Barat, 31900 Kampar, Perak, Malaysia

* Corresponding author: ongst@utar.edu.my; ongst_utar@yahoo.com



INTRODUCTION

Water pollution can bring critical impacts to the environment. Major source of this pollution comes from the textile industry due to the presence of dyes in the effluents that cannot be completely eliminated before discharge into the river or ocean. Other than dyes, large quantity of heavy metals, surfactants and dissolved solids were also found in the wastewater from the dyeing and finishing processes. The elimination of colours in effluents have become a major concern for both the industry as well as the society [1]. There is about 10 to 15 % of used dyes that released into the environment from the effluent from textile, paper and plastic industries as massive amount of dyes are utilized in these industries [2].

Quite often, appreciable amount of dyes remained in the effluent due to the inefficiencies of the conventional wastewater treatment. The treatment of wastewater cannot depend solely on biodegradation process because the dye itself and its degradation product may be toxic and carcinogenic [3]. The photosynthesis process is also affected by the coloured effluents which can decrease the penetration of light [4].

There are a lot of methods that can be used to eliminate the pollutants such as membrane separation process, chemical oxidation, coagulation, photocatalysis and electrochemical processes. Nevertheless, these methods are not preferred since there are many limitations and disadvantages [5]. Various studies have concluded that the most efficient technique to eliminate a variety of dyes is by the adsorption of dyes onto activated carbons. But due to the high generation cost, alternative adsorbents had been investigated to replace it [6,7].

The more realistic and low-cost method to remove various contaminants is by adsorption using agricultural by-products such as rice husk, peanut husk, palm kernel fibre and palm shell [5]. The conversion of agricultural waste to adsorbent is a great way to increase the value of these waste instead of disposal to landfill which bring ecological and economical concern [8]. Hydroxyl, amino and carboxyl groups present on the surface of agricultural wastes provide them great biosorption potential and can be further improved through various treatments [9].

The world total production of peanut is around 50 million metric tons in 2021. The largest manufacturer of peanut was China which contributes about 36 % (18 million metric tons) of the total production and followed by India [10]. Peanut kernels take up 70 % of the total weight while the rest 30 % are from the peanut husks. The major components in peanut husks are cellulose, hemicelluloses and lignin [11].

There are two major groups of dye which are anionic dye and cationic dye. MB is a cationic dye commonly used to colour textile, paper and wood. It is known as a cationic dye because it is able to dissociates into positively charged compound [2]. They are bright and high colour intensity dyes, therefore even when the concentrations are low, basic dyes are highly visible [12]. The elimination of MB has been attracting the interest of researchers because among all classes of dyes, cationic dyes are generally more toxic compared to others. Furthermore, the removal of dye can be challenging due to their unique properties such as stable and resistant to light and aerobic digestion and can act as an oxidizing agent [2].

RESULTS AND DISCUSSION

Characterization of Adsorbent

Fourier Transform Infrared Spectroscopy (FTIR) Analysis. The presence of functional groups on peanut husks before and after adsorption of MB was analysed using FTIR spectrophotometer at the wavenumber range of 4000 – 400 cm^{-1} . From the spectrum before adsorption (spectrum not shown), a strong and broad peak observed at 3411 cm^{-1} was due to the vibrations of hydroxyl groups of alcohols, carboxylic acids and phenols. The medium peak at 2929 cm^{-1} represented the sp^3 C-H stretch while the peak at 1735 cm^{-1} was the C=O stretching vibrations of esters. The presence of hemicelluloses was signified by a medium peak at 1639 cm^{-1} because it is the characteristic band of stretching carbonyl groups of hemicelluloses [13]. The CH_2 bending was represented by the medium peak at 1429 cm^{-1} . There were two medium peaks observed at 1377 and 1319 cm^{-1} which are the O-H bending of phenols. The broad and strong overlapping bands from 1157 - 1035 cm^{-1} indicated the C-O stretching vibrations and these absorptions may have occurred due to the phenolic structure [14].

By comparing the spectrum before and after adsorption, there was no big difference in the shape and intensity of the peaks. The O-H stretching vibrations at 3411 cm^{-1} shifted to 3421 cm^{-1} . The sp^3 C-H stretching band was shifted from 2929 to 2933 cm^{-1} . The CH_2 bending shifted from wavenumber 1429 to 1431 cm^{-1} . This could be related to the limitations in the sensitivity the instrument. In some of the previously reported works involving the adsorption studies by using other agro-based materials, the FTIR spectra before and after the adsorption process were also were similar to each other [15-17].

Scanning Electron Microscopy (SEM) Analysis. Figures 1(a) and 1(b) showed the SEM micrographs of peanut husks before and after adsorption of MB, respectively. A smoother and more even surface was observed in the micrograph of peanut husks before adsorption of dye. The surface of peanut

husks after adsorption was uneven and rougher compared to the raw peanut husks. This is most probably due to the adhesion and agglomeration of MB dye molecules onto the peanut husks, which also shown that peanut husks have the ability to remove MB from solution by adsorption.

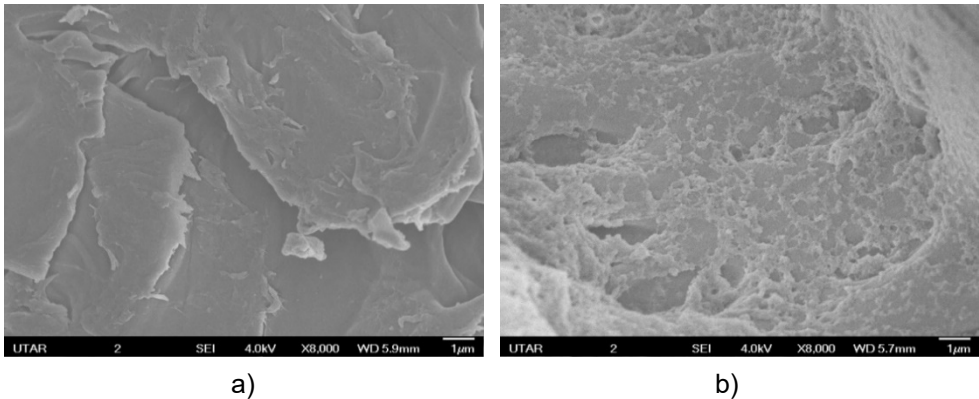


Figure 1 SEM micrograph of peanut husks with 8000× magnification: a) before adsorption b) after adsorption

Atomic Force Microscopy (AFM) Analysis. The AFM micrographs in Figures 2(a) and 2(b) presented the surface topology of peanut husks before and after adsorption of MB, respectively. The dark areas were more evident on the surface of peanut husks before the adsorption. The distribution of dark and light areas was quite average. The surface of peanut husks after adsorption was smoother because the pores were saturated with MB dye molecules. Besides, it can be observed that a lighter colour surface was in dominant indicating that they were almost at the same level. These results further confirm the ability of peanut husks to adsorb MB.

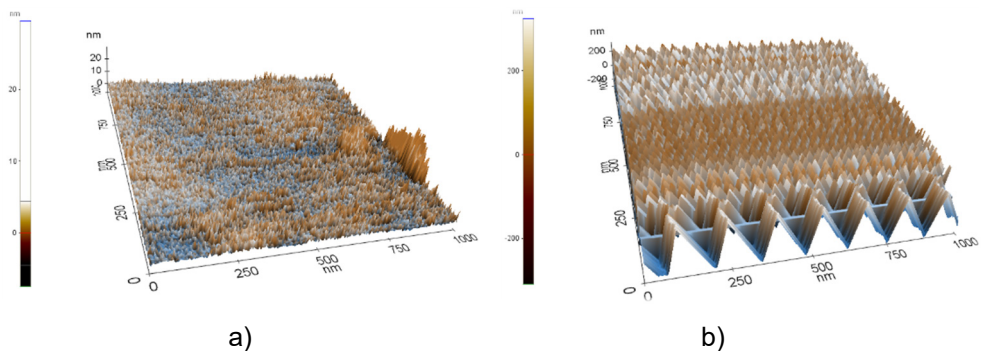


Figure 2. AFM micrograph of peanut husks a) before adsorption of MB; b) after adsorption of MB

Batch Adsorption Studies

Effect of contact time and initial dye concentration. Figure 3 showed the percentage uptake of three different concentrations of MB: 25, 50 and 100 mg/L by peanut husks from 0 to 240 minutes. The trend of adsorption was similar for all three concentrations of MB. The percentage uptake increases as contact time increases and the adsorption rate was high in the first 30 minutes. Then, percentage uptake of dye increases gradually until the equilibrium was achieved after 180 minutes.

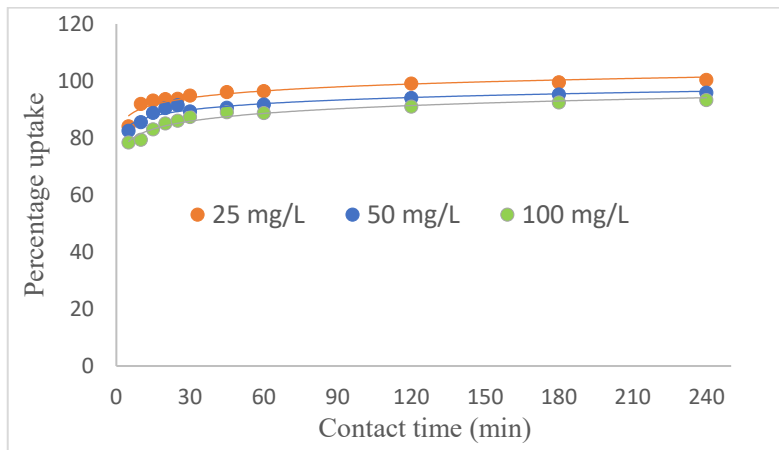


Figure 3. Effect of contact time and initial dye concentration on percentage uptake of MB

The adsorption was rapid in the beginning of the experiment because of large number of unoccupied adsorption sites available on adsorbent surface and the electrostatic attraction between surface of adsorbent, which is peanut husks and adsorbates, MB dye solution. After the first 30 minutes, the rate of adsorption decelerates and the percentage uptake reached its maximum after 180 minutes because all the adsorption sites were fully occupied by dye molecules [18]. As seen from Figure 3, the percentage uptake of MB decreases as the concentration of MB increases. When MB concentration is high, number of dye molecules available for binding also increases. However, the number of vacant binding sites remain the same and binding sites are easily saturated with dye molecules. The amount of dye molecules to binding sites ratio is large causing dye molecules to have lower chances to interact with binding sites. Hence, resulting in the decrease in percentage uptake of dye [19,20].

Effect of pH. Figure 4 illustrated the percentage uptake of MB at various pH values. The adsorption of dye can be greatly influenced by the surface charges of adsorbent and also the dye molecules. MB is a cationic dye which will be attracted to the negatively charged surface. So, the percentage uptake of MB will be enhanced when the surface of peanut husks is more negatively charged.

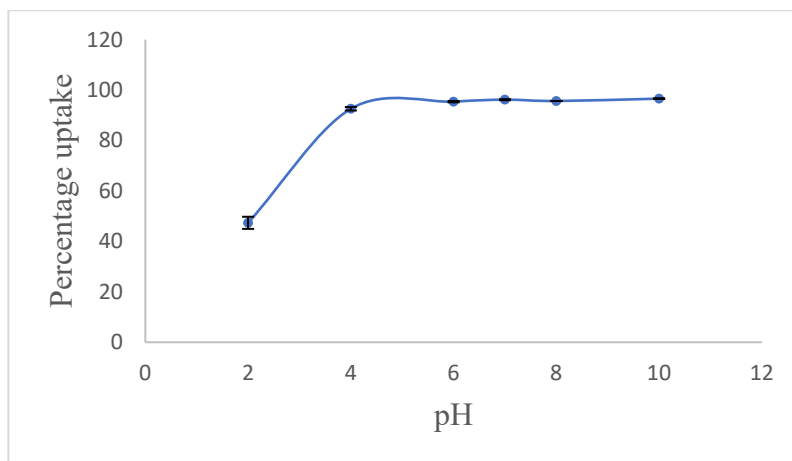


Figure 4. Effect of pH on percentage uptake of MB

The range of pH 4 to 10 was the optimum pH for maximum MB uptake. At pH 2 which is a highly acidic condition, only 47.36 % of MB has been removed. The percentage uptake has increased drastically from 47.36 % to 92.58 % at pH 4. The pH_{pzc} of peanut husks was determined to be 4.7. At pH 6, where $pH > pH_{pzc}$, the percentage uptake increased to 95.40 % and remained almost constant until pH 10 which is 96.60 %, the highest percentage uptake. At $pH < pH_{pzc}$, the functional groups on the adsorbent surface will undergo protonation and become positively charged with the addition of protons. Therefore, the electrostatic repulsion between positively charged peanut husks surface and cationic MB molecules resulted in the decrease in adsorption of dye molecules. At $pH > pH_{pzc}$, the situation reversed where the percentage uptake of cationic MB dye increased. The peanut husk will have a negatively charged surface when $pH > pH_{pzc}$ because positively charged groups on the adsorbent start to deprotonate. This condition favours the adsorption of cationic MB dye because of the electrostatic attraction between peanut husks surface that is having negative charge and positively charged MB dye molecules [5,21].

Effect of adsorbent dosage. The percentage uptake of MB by using different amount of peanut husks was presented in Figure 5. The lowest percentage uptake was observed for 0.01 g of peanut husks which was 86.51 % and the highest percentage uptake of MB dye, 94.82 % was observed for 0.06 g of peanut husks. According to Salleh et al. [5], this is due to increase in number of adsorption sites available for the attachment of dye molecules as adsorbent dosage rises. The amount of dye molecules to binding sites ratio is small causing dye molecules to have higher chances to interact with the binding sites.

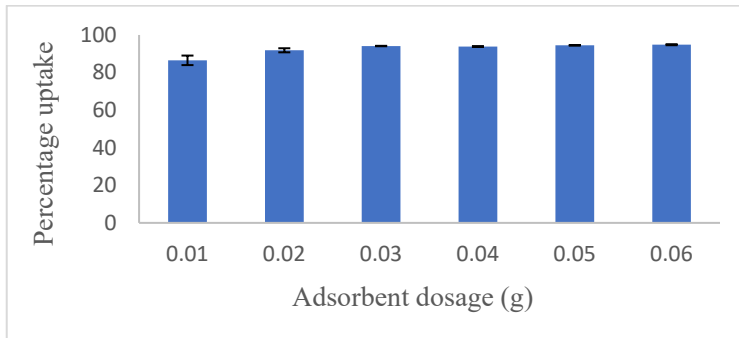


Figure 5. Effect of adsorbent dosage on percentage uptake of MB

Nonetheless, a slight decrease of percentage uptake at 0.04 g was noticed. Sometimes, an increase in dosage may lead the formation of aggregates between adsorbents that blocked the adsorption sites. Aggregation of adsorbents may cause the reduction in effective surface area and an increase in diffusional path length, which subsequently cause a reduction in the percentage uptake [22,23].

Adsorption Kinetic Studies

Pseudo-First-Order Kinetic Model. Pseudo-first-order kinetic model assumes that the number of vacant binding sites remained and rate change of concentration of surface adsorption sites are directly proportional to each other [24]. The linear pseudo-first-order model equation is presented as:

$$\log(q_e - q_t) = \log q_e - \frac{k_1}{2.303} t \quad (1)$$

where

q_e = Amount of adsorbate adsorbed at equilibrium (mg/g)

q_t = Amount of adsorbate adsorbed at time t (mg/g)

k_1 = Pseudo-first-order kinetics rate constant (min^{-1})
 t = Time in minutes

In many cases, the kinetics of adsorption by biological materials are described by pseudo-first order kinetics and therefore the adsorption data was analysed using this model. However, in this study, it was found that pseudo-first-order equation did not fit well for the whole range of concentrations studied. Besides, the equilibrium adsorption capacities calculated from this model gave higher deviations as compared to those determined based on pseudo-second-order kinetics model (Table 1). The low R^2 values obtained based on this pseudo-first-order equation also suggested that this kinetic model was not suitable to depict the adsorption of MB by peanut husks.

Table 1. Pseudo-first and pseudo-second-order kinetics model parameters

Initial concentration of MB (mg/L)	Pseudo-first-order			Pseudo-second-order				Experimental q_e (mg/g)
	q_e (mg/g)	k_1 (min^{-1})	R^2	q_e (mg/g)	h (mg/g·min)	k_2 (g/mg·min)	R^2	
25	14.0540	0.09719	0.7805	16.5622	10.8578	0.03870	0.9999	16.5725
50	30.2691	0.10179	0.7289	32.0889	21.2766	0.02071	0.9999	31.7514
100	67.7018	0.09880	0.7362	60.4014	32.0513	0.00831	0.9998	61.3936

Pseudo-Second-Order Kinetic Model. Pseudo-second-order kinetic model assumes that the square of number of unoccupied binding sites remained and the rate change of concentration of surface adsorption sites are directly proportional to each other. In this kinetic model, the rate-determining step is a chemisorption because the electrons exchanging or sharing between adsorbate and adsorbent involving valency forces [25]. The linear pseudo-second-order model equation is presented as:

$$\frac{t}{q_t} = \frac{1}{h} + \frac{t}{q_e} \quad (2)$$

$$h = k_2 q_e^2 \quad (3)$$

where

q_e = Amount of adsorbate adsorbed at equilibrium (mg/g)
 q_t = Amount of adsorbate adsorbed at time t (mg/g)
 k_2 = Pseudo-second-order kinetics rate constant (g/mg min)
 t = Time in minutes
 h = Initial adsorption rate (mg/g min)

Graph of t/q_t against t of 25, 50 and 100 mg/L of MB solution was plotted and the y-intercept the graph can be used to determine h value whereas gradient can be used to calculate q_e (Figure not shown). Then, by using equation 3, the value of k_2 can be calculated. The R^2 values for 25, 50 and 100 mg/L of MB were 0.9999, 0.9999 and 0.9998, respectively (Table 1). All R^2 values are very close to unity, also, the experimental q_e and the calculated q_e are having similar values. The experimental data fitted well into the pseudo-second-order kinetic model and this model was said to correlate well with the experimental data. This model was appropriate to be used to describe the adsorption of MB by peanut husks. Therefore, it is suggested that the adsorption process may be involving a chemisorption process. Figure 6 showed that the experimental data represented by the symbol agreed well with the theoretically generated curves.

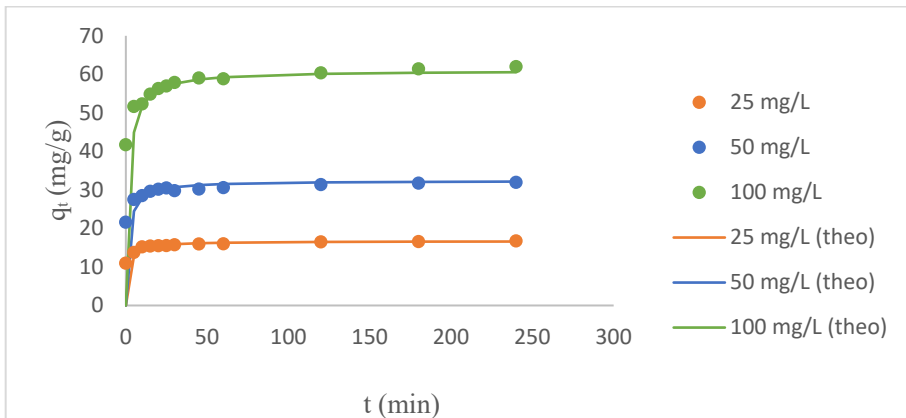


Figure 6. Comparison between theoretical (line) and experimental (symbol) data

Adsorption Isotherm Studies

Langmuir Isotherm Model. Langmuir isotherm model assumes that each adsorption site can be occupied by only one adsorbate molecule and the number of adsorption sites are fixed. There are no interactions between the adsorbate molecules, the adsorbate molecules are adsorbed onto the binding sites chemically. It is a monolayer adsorption that takes place on homogeneous surfaces [26]. The Langmuir model equation is written as:

$$q_e = \frac{q_m K_L C_e}{1 + K_L C_e} \quad (4)$$

By rearranging equation 4, the Langmuir model equation in linear form is written as:

$$\frac{C_e}{q_e} = \frac{C_e}{q_m} + \frac{1}{K_L q_m} \quad (5)$$

where

- q_e = Amount of adsorbate adsorbed at equilibrium (mg/g)
 q_m = Maximum adsorption capacity (mg/g)
 K_L = Langmuir constant related to energy of adsorbent (L/mg)
 C_e = Concentration of adsorbate at equilibrium (mg/L)

The gradient and y-intercept obtained from the linear plot can be used to calculate q_m and K_L values, respectively and they were found to be 117.6471 mg/g and 0.1540 L/mg, respectively (Table 2). Based on the q_m value, it is suggested that peanut husk is an attractive adsorbent with considerable high adsorption capacity towards MB as compared to some previously reported works [27-29].

Freundlich Isotherm Model. Freundlich isotherm model made a few assumptions that physicochemical sorption takes place on heterogeneous surfaces and it is a multilayer adsorption process. The interactions between the adsorbate molecules are present [30]. The Freundlich model equation is written as:

$$q_e = K_F C_e^{\frac{1}{n}} \quad (6)$$

By rearranging equation 6, the Freundlich model equation in linear form is written as:

$$\log q_e = \frac{\log C_e}{n} + \log K_F \quad (7)$$

where

- q_e = Amount of adsorbate adsorbed at equilibrium (mg/g)
 C_e = Concentration of adsorbate at equilibrium (mg/L)
 n = Freundlich constant for intensity
 K_F = Freundlich constant for adsorption capacity

Figure 7 presented the graph of $\log q_e$ against $\log C_e$ for adsorption of MB. By using the gradient obtained from the plot, the n value can be calculated. Besides, K_F value was determined from y-intercept of the plot. Values of n and K_F were determined to be 1.7343 and 18.3147, respectively. The R^2 value was 0.9927 which was very close to unity (Table 2). This shows that the equilibrium adsorption data is best fitted with Freundlich isotherm model and implies that the nature of MB adsorption on peanut husks is a multilayer, physicochemical sorption that takes place on heterogeneous surfaces.

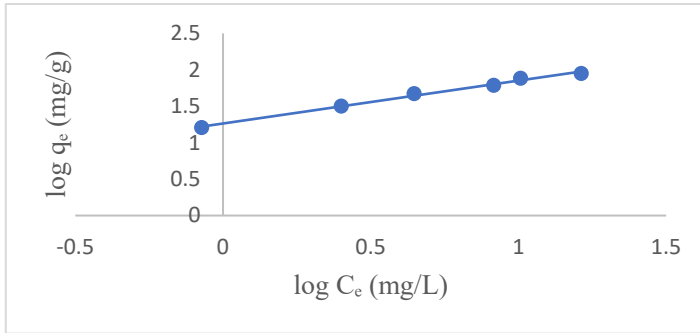


Figure 7. Freundlich isotherms for adsorption of MB

Brunauer-Emmett-Teller (BET) Isotherm Model. The assumptions made in BET isotherm model are the heat of adsorption is the same for all adsorbed layers except the first layer and first layer adsorbates will have the strongest interaction with the adsorbent compared to subsequent layers. It is a multilayer sorption takes place on homogeneous surface and number of adsorption sites are fixed [31]. The equation of BET model is written as:

$$q_e = \frac{K_B C_e q_m}{(C_s - C_e) \left[1 + (K_B - 1) \left(\frac{C_e}{C_s} \right) \right]} \quad (8)$$

By rearranging equation 8, the BET model equation in linear form is illustrated as:

$$\frac{C_e}{(C_s - C_e) q_e} = \left(\frac{K_B - 1}{K_B q_m} \right) \left(\frac{C_e}{C_s} \right) + \frac{1}{K_B q_m} \quad (9)$$

where

- C_e = Concentration of adsorbate at equilibrium (mg/L)
- C_s = Saturation concentration of solute (mg/L)
- q_e = Amount of adsorbate adsorbed at equilibrium (mg/g)
- q_m = Amount of adsorbate in forming a complete monolayer (mg/g)
- K_B = BET constant describing the energy of adsorbate-adsorbent interaction

The gradient and y-intercept from the linear plot of C_e/(C_s-C_e)q_e against C_e/C_s were utilized to determine K_B and q_m values (Figure not shown). The value of K_B was 431 while q_m value was 116.0093 mg/g. The C_s value was determined by calculating the maximum amount of adsorbate which is MB that can be dissolved in minimum volume of solvent. The C_s value of MB was 2250 mg/L. Table 2 indicated all the R² values and parameters obtained from Langmuir, Freundlich and BET isotherm models. The R² value for all

three isotherm models were very high, however, the Freundlich isotherm model showed a slightly better fit to the experimental data compared to Langmuir and BET models. This suggests that the binding sites on peanut husks are mostly heterogeneous and since peanut husks are biosorbents there may have various kind of surface adsorption sites [32].

Table 2. Values obtained from Langmuir, Freundlich and BET isotherm models

Langmuir isotherm		Freundlich isotherm		BET isotherm	
q_m (mg/g)	117.6471	n	1.7343	q_m (mg/g)	116.0093
K_L (L/mg)	0.1540	K_F	18.3147	K_B	431
R^2	0.9709	R^2	0.9927	R^2	0.9717

Optimization studies

Plackett-Burman (PB) Design. The most important factors that can give a significant impact to percentage uptake of dyes can be determined using PB [33]. Contact time, adsorbent dosage, pH and initial dye concentration were examined using PB design to select the significant factors that bring strong impact to the adsorption process. Twelve runs with different experimental conditions were performed and an ANOVA table was generated based on the experimental results. Table 3 presented the ANOVA results of PB. This model has p-value of 0.0010 which indicated that it is significant because p-value < 0.05. Out of the four factors, adsorbent dosage, pH and contact time were identified as the significant factors except initial dye concentration with p-value of 0.6416 which is larger than 0.05.

Table 3. ANOVA of PB for adsorption of Methylene Blue by peanut husks

Source	Sum of Squares	df	Mean Square	F Value	p-value
Model	11560.91	4	2890.23	17.01	0.0010
A-Contact time	1441.90	1	1441.90	8.48	0.0226
B-pH	6782.06	1	6782.06	39.91	0.0004
C-Initial dye concentration	40.19	1	40.19	0.24	0.6416
D-Dosage	3296.77	1	3296.77	19.40	0.0031
Residual	1189.55	7	169.94		
Lack of Fit	1189.55	6	198.26		

R-Squared 0.9067

Predicted R-Squared 0.7258

Adjusted R-Squared 0.8534

Adequate Precision 12.6303

Verification of Plackett-Burman Design Models. Validation of this model was done by employing function of desirability. The experimental condition with highest desirability generated by the software were performed.

Response Surface Methodology (RSM). The effect of different variables on MB uptake were studied using RSM and the variables involved were adsorbent dosage, pH and contact time. RSM generated 20 different sets of experiment and an ANOVA table was generated based on the experimental results. The ANOVA of RSM were presented in Table 4. The relationship between the three significant factors and the percentage uptake of MB were illustrated in the modified cubic model shown below:

Percentage Uptake

$$= 95.65 + 5.13 * A + 24.89 * B + 11.01 * C - 0.63 * AB - 0.43 * AC - 8.46 * BC - 4.92 * A^2 - 23.21 * B^2 - 3.95 * C^2$$

where

- A = Contact time
 B = pH
 C = Adsorbent dosage

The p-value of model of experiment is smaller than 0.0001 as seen in Table 4 indicated that it was significant. Similarly, the p-value for the three significant factors were also less than 0.05. The high R² value which was 0.9890 showed that the experimental results agreed well with the expected results. The adjusted R² was 0.9791 while the predicted R² was 0.8378.

Table 4. ANOVA of RSM for adsorption of Methylene Blue by peanut husks

Source	Sum of Squares	df	Mean Square	F Value	p-value
Model	12491.99	9	1388.00	99.94	< 0.0001
A-Contact time	263.38	1	263.38	18.96	0.0014
B-pH	6194.90	1	6194.90	446.05	< 0.0001
C-Dosage	1212.26	1	1212.26	87.29	< 0.0001
AB	3.16	1	3.16	0.23	0.6439
AC	1.45	1	1.45	0.10	0.7536
BC	572.85	1	572.85	41.25	< 0.0001
A ²	66.60	1	66.60	4.80	0.0534
B ²	1481.26	1	1481.26	106.65	< 0.0001
C ²	42.88	1	42.88	3.09	0.1094
Residual	138.88	10	13.89		
Lack of Fit	138.88	5	27.78		

R-Squared 0.9890 Predicted R-Squared 0.8378

Adjusted R-Squared 0.9791 Adequate Precision 34.0345

They agreed with each other reasonably. Coefficient of variance (CV) was determined to be 4.68 % which showed that the reliability and precision of this model is high. The adequate precision obtained was 34.0345 which indicated an adequate signal because it is greater than 4. Ratio of signal to noise can be measured by adequate precision.

Figure 8 presented the 3D surface plot for the correlation between percentage uptake of MB, contact time and pH. Maximum dye uptake was observed at long contact time and high pH. As contact time increases, only a slight change in the percentage removal was observed because the equilibrium time has been reached. The maximum adsorption capacity of adsorbent can be determined at equilibrium time [33]. The percentage uptake increases as pH increases and remained almost constant after pH 6. High pH condition favours the adsorption of cationic MB dye because the positively charged groups on the adsorbent start to deprotonate and leads to high electrostatic attraction between peanut husks surface and cationic MB molecules.

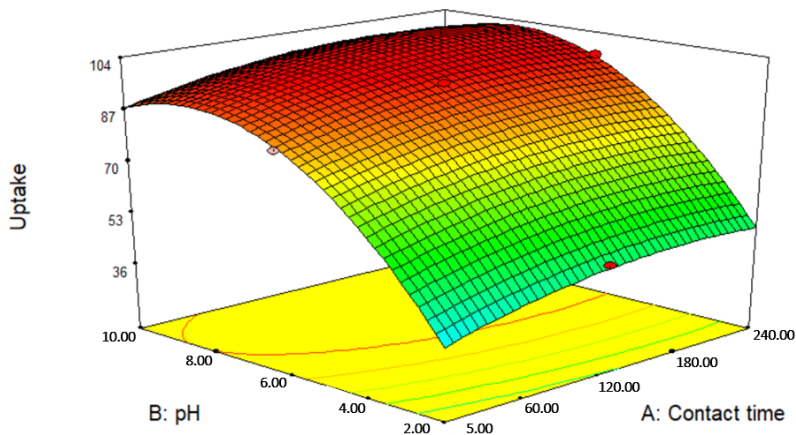


Figure 8. 3D surface plot for the percentage uptake of MB by peanut husks as a function of pH and contact time at 50 mg/L of initial MB concentration

Figure 9 illustrated the 3D surface plot for the relationship between percentage uptake of MB, adsorbent dosage and contact time. The trend of percentage uptake versus contact time is very similar to the one observed in Figure 8. As adsorbent dosage increases, the uptake of MB also increases. This is because there are more surface area and increasing number of vacant binding sites for attachment of dye molecules.

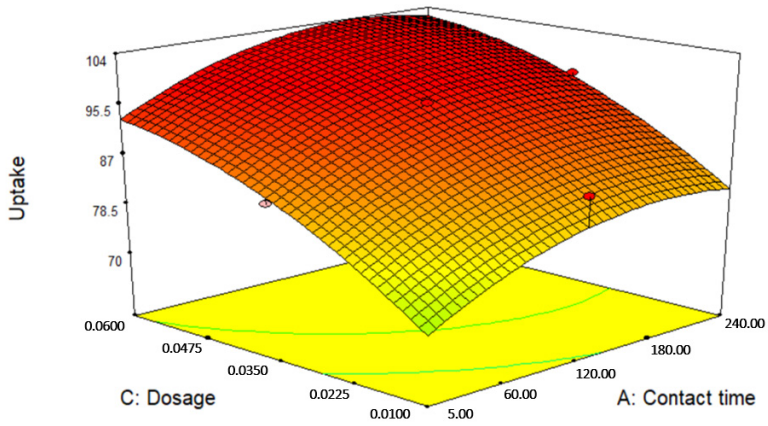


Figure 9. 3D surface plot for the percentage uptake of MB by peanut husks as a function of adsorbent dosage and contact time at 50 mg/L of initial MB concentration

Figure 10 illustrated the 3D surface plot for the relationship between percentage uptake of MB, adsorbent dosage and pH. The percentage uptake increases as adsorbent dosage increases and has the same pattern as observed in Figure 9. The trend of percentage uptake versus pH is also very similar to the one observed in Figure 8 where the percentage uptake remained almost constant after pH 6.

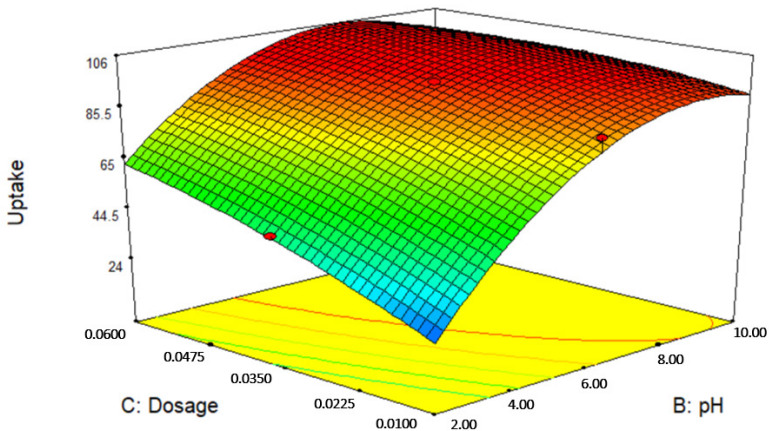


Figure 10. 3D surface plot for the percentage uptake of MB by peanut husks as a function of adsorbent dosage and pH at 50 mg/L of initial MB concentration

Verification of Response Surface Methodology Models. The equation generated was validated by performing the experiment under conditions with highest desirability. Percentage of differences calculated between expected and experimental results for each set of experiment was within 0.05 - 5.16 %. The percentage differences are considered low and this indicates that the generated model equation is valid.

CONCLUSIONS

Peanut husks were found to be a potential adsorbent to remove MB dye solution in this study. In FTIR analysis, there was no significant shift before and after adsorption of dye showing that the functional groups on peanut husks remained the same. SEM and AFM analysis further confirmed that there is adsorption of MB dye occurred on peanut husks by observing the surface morphology after adsorption and compared with peanut husks before adsorption. A good fit of experimental data into pseudo-second-order kinetic model suggested that chemisorption process was involved in this study with R^2 close to unity. In the isotherm study, compared to Langmuir and BET models, Freundlich model with R^2 of 0.9927 showed a slightly better fit to the experimental data. PB was performed to determine the significant factor in the removal of MB by peanut husks. Adsorbent dosage, pH and contact time were determined as the significant factors in this experiment. The optimum level of each significant variable to reach the maximum percentage uptake of dye was determined using RSM and a modified cubic model equation was generated. The percentage of differences calculated for each set of experiment was below 6 %. Optimum condition was reached at 120 minutes of contact time, pH 10 and 0.035 g of adsorbent.

EXPERIMENTAL SECTION

Preparation of adsorbent

Peanut husks were chosen as the adsorbent to be studied in this project. The peanut husks and kernels were first separated. The husks were washed thoroughly with water. Then, the husks were sun-dried for a few days and followed by drying in an oven for 24 hours at 65 °C to ensure the moisture was completely removed. The dry peanut husks were grounded with a blender into powder form and screened through a 1 mm sieve. The samples were then stored in a glass media bottle with silica gel.

Preparation of Methylene Blue solution

MB solution was chosen as the adsorbate in this study. The molecular weight of MB is 319.85 g/mol and its molecular formula is $C_{16}H_{18}ClN_3S$. The stock solution of 1000 mg/L was prepared by using a 1 L volumetric flask. Then, it was stored in a dark place to prevent degradation from direct sunlight. Dilution technique was then applied for the preparation of working solution.

Characterization of adsorbent

Fourier Transform Infrared Spectroscopy. The functional groups present on peanut husks can be studied using FTIR spectrometer model Spectrum RX1. The dried peanut husks were ground with KBr powder to a homogenous mixture and vacuum pressed into pellets for analysis. Both peanut husks before and after adsorption of dye were analysed at the wavenumber ranging from 4000 – 400 cm^{-1} .

Scanning Electron Microscopy. The surface morphology of peanut husks before and after adsorption of dye were studied at emissions current of 4.0 kV using SEM model JEOL-JSM-6701F.

Atomic Force Microscopy. The surface topology of peanut husks before and after adsorption of dye were studied using AFM model Park XE-70 AFM.

Batch experiments

A 0.03 g of peanut husks was added into a centrifuge tube containing 20 mL of MB solution. The mixture was agitated for 3 hours with 150 rpm on an orbital shaker. A control set without peanut husks was performed simultaneously to prove that the dye adsorption is because of the presence of peanut husks instead of the centrifuge tube wall. The mixtures were then centrifuged at 7000 rpm for phase separation. Dye concentration of supernatant was analysed at 664 nm which is the maximum wavelength of MB by using a UV-Vis spectrophotometer. All batch experiments were done in duplicate and mean results were obtained. Equation below was used to calculate the percentage uptake of dye:

$$\text{Percentage uptake} = \frac{C_o - C_t}{C_o} \times 100 \%$$

where

C_o = Initial MB concentration (mg/L)

C_t = MB concentration at time, t (mg/L)

The effect of initial dye concentration was examined by using 20 mL of 25 mg/L of MB solution with 0.03 g of peanut husks. The experiment was repeated with 50 and 100 mg/L of MB solution. For each solution, at predetermined time intervals which are 5, 10, 15, 20, 25, 30, 45, 60, 120, 180 and 240 minutes, the absorbance of dye was measured and the dye concentration was calculated.

HCl or NaOH solution of 0.01, 0.1 and 1 M were added dropwise into the solution to adjust it to desired pH. A 50 mg/L of MB solution with pH ranging from 2 to 10 was prepared for this study. The solution was then placed on the orbital shaker at 150 rpm for 3 hours to reach the equilibrium.

Different amount of adsorbent ranging from 0.01 g - 0.06 g was added into 50 mg/L MB dye solution, respectively. The mixture was then subjected to 3 hours of contact time for the adsorption process to reach equilibrium to determine the effect of adsorbent dosage on adsorption process.

Optimization studies

Plackett-Burman design was performed to eliminate the insignificant factors in the adsorption of dye. Contact time, adsorbent dosage, pH and initial dye concentration were studied in this analysis. The interaction between each significant factor and their optimum levels can be identified by using Response Surface Methodology. The factors involved were pH, contact time and adsorbent dosage. All experiments were done in duplicates and the mean absorbance were obtained. The Design Expert Version 7.1.3 was used in the statistical and experimental design of the adsorption process.

ACKNOWLEDGEMENTS

The financial support and research facilities by Universiti Tunku Abdul Rahman are acknowledged.

REFERENCES

1. N. Kannan; M.M. Sundaram; *Dyes Pigm.*, **2001**, *51*, 25-40
2. S.L. Lee; S.W. Liew; S.T. Ong; *Acta Chim. Slov.*, **2016**, *63*, 144-153
3. S.L. Chan; Y.P. Tan; A. H. Abdullah; S.T. Ong; *J. Taiwan Inst. Chem. Eng.*, **2016**, *61*, 306-315
4. S.T. Ong; C.K. Seou; *Desalination Water Treat.*, **2013**, *52*, 7673-7684
5. M.A.M. Salleh; D.K. Mahmoud; W.A.W.A. Karim; A. Idris; *Desalination*, **2011**, *280*, 1-13

6. S.T. Ong; E.H. Tay; S.T. Ha; W.N. Lee; P.S. Keng; *Int. J. Phys. Sci.*, **2009**, *4*, 683-690
7. S.T. Ong; W.N. Lee; P.S. Keng; Y.T. Hung; S.T. Ha; *Int. J. Phys. Sci.*, **2010**, *5*, 582-595
8. R. Malik; D.S. Ramteke; S.R. Wate; *Indian J. Chem. Technol.*, **2006**, *13*, 319-328
9. S. Sadaf; H.N. Bhatti; *J. Taiwan Inst. Chem. Eng.*, **2013**, *45*, 541-553
10. *World Agricultural Production*, United States Department of Agricultural, USA, **2022**, pp. 1-43
11. Inamuddin; A. Mohammad; A.M. Asiri; *Inorganic Pollutants in Wastewater: Methods of Analysis, Removal and Treatment*, Materials Research Forum LLC, Millersville, USA, **2017**, p. 195
12. L. Zafar; A. Khan; U. Kamran; S. Park; H.N. Bhatti; *Surf. Interfaces*, **2022**, *31*, 101897
13. B. Kumar; U. Kumar; *Korean J. Chem. Eng.*, **2015**, *32*, 1655-1666
14. S. Ricordel; S. Taha; I. Cisse; G. Dorange; *Sep. Purif. Technol.*, **2001**, *24*, 389-401
15. L. Das; P. Das; A. Bhowal, C. Bhattacharjee; *J. Environ. Manage.*, **2020**, *276*, 111272.
16. C.I. Tay; S.T. Ong; *J. Phys. Sci.*, **2019**, *30*, 137-156.
17. H.Y. Gan, L.E. Leow, S.T. Ong; *Acta Chim. Slov.*, **2017**, *64*, 144-158.
18. M.U. Farooq; M.I. Jalees; A. Iqbal; N. Zahra; A. Kiran; *Desalination Water Treat.*, **2019**, *160*, 333-342
19. D. Özer; G. Dursun; A. Özer; *J. Hazard. Mater.*, **2007**, *144*, 171-179
20. N.A. Taha; A. El-Maghraby; *Glob. Nest J.*, **2015**, *18*, 25-37
21. W. Zou; H. Bai; S. Gao; K. Li; X. Zhao; R. Han; *Desalination Water Treat.*, **2012**, *49*, 41-56
22. N. Besharati; N. Alizadeh; S. Shariati; *J. Mex. Chem. Soc.*, **2018**, *62*, 110-124
23. N. Tahir; H.N. Bhatti; M. Iqbal; S. Noreen; *Int. J. Biol. Macromol.*, **2017**, *94*, 210-220
24. S. Lagergren; *Kungl. Svenska Vetenskapsakad. Handl.*, **1898**, *24*, 1-39
25. Y.S. Ho; G. McKay; *Process Biochem.*, **1999**, *34*, 451-465
26. I. Langmuir; *J. Am. Chem. Soc.*, **1918**, *40*, 1361-1403
27. L. Lonappan; T. Rouissi; R.K. Das; S.K. Brar; A.A. Ramirez; M. Verma; R.Y. Surampalli; J.R. Valero; *Waste Manag.*, **2016**, *49*, 537-544
28. L. Meili; P.V.S. Lins; M.T. Costa; R.L. Almeida; A.K.S. Abud; J.I. Soletti; G.L. Dotto; E.H. Tanabe; L. Sellaoui; S.H.V. Carvalho; A. Erto; *Prog. Biophys. Mol. Biol.*, **2019**, *141*, 60-71
29. T.C. Egbosiuba; A.S. Abdulkareem; A.S. Kovo; E. A. Afolabi; J.O. Tijani; M. Auta; W.D. Roos; *Chem Eng Res Des.*, **2020**, *153*, 315-336
30. H.M.F. Freundlich; *J. Phys. Chem.*, **1906**, *57*, 385-471
31. S. Brunauer, P.H. Emmett, E. Teller; *J. Am. Chem. Soc.*, **1938**, *60*, 309-319
32. S.T. Ong; C.K. Lee; Z. Zainal; *Bioresour. Technol.*, **2007**, *98*, 2792-2799
33. S.T. Ong; E.C. Khoo; P.S. Keng; S.L. Hii; S.L. Lee; Y.T. Hung; S.T. Ha; *Desalination Water Treat.*, **2011**, *25*, 310-318

